Mon. Not. R. Astron. Soc. **000**, 000–000 (0000) Printed 2 February 2022 (MN LATEX style file v2.2)

The initial-final mass relationship of white dwarfs revisited: effect on the luminosity function and mass distribution

S. Catalán[1,2⋆], J. Isern[1,2], E. García–Berro[1,3] and I. Ribas[1,2]
[1] *Institut d'Estudis Espacials de Catalunya, c/ Gran Capità 2–4, 08034 Barcelona, Spain*
[2] *Institut de Ciències de l'Espai, CSIC, Facultat de Ciències, Campus UAB, 08193 Bellaterra, Spain*
[3] *Departament de Física Aplicada, Escola Politècnica Superior de Castelldefels, Universitat Politècnica de Catalunya, Avda. del Canal Olímpic s/n, 08860 Castelldefels, Spain*

arXiv:0804.3034v1 [astro-ph] 18 Apr 2008

2 February 2022

ABSTRACT
The initial-final mass relationship connects the mass of a white dwarf with the mass of its progenitor in the main-sequence. Although this function is of fundamental importance to several fields in modern astrophysics, it is not well constrained either from the theoretical or the observational points of view. In this work we revise the present semi-empirical initial-final mass relationship by re-evaluating the available data. The distribution obtained from grouping all our results presents a considerable dispersion, which is larger than the uncertainties. We have carried out a weighted least-squares linear fit of these data and a careful analysis to give some clues on the dependence of this relationship on some parameters such as metallicity or rotation. The semi-empirical initial-final mass relationship arising from our study covers the range of initial masses from 1.0 to 6.5 $M_{\odot}$, including in this way the low-mass domain, poorly studied until recently. Finally, we have also performed a test of the initial-final mass relationship by studying its effect on the luminosity function and on the mass distribution of white dwarfs. This was done by using different initial-final mass relationships from the literature, including the expression derived in this work, and comparing the results obtained with the observational data from the Palomar Green Survey and the Sloan Digital Sky Survey (SDSS). We find that the semi-empirical initial-final mass relationship derived here gives results in good agreement with the observational data, especially in the case of the white dwarf mass distribution.

Key words: white dwarfs — stars: evolution, luminosity function, mass function — open clusters and associations: general.

1 INTRODUCTION

The initial-final mass relationship of white dwarfs links the mass of a white dwarf with that of its progenitor in the main-sequence. This function is of paramount importance for several aspects of modern astrophysiscs such as the determination of the ages of globular clusters and their distances, the study of the chemical evolution of galaxies, and also to understand the properties of the Galactic population of white dwarfs. However, we still do not have an accurate measurement of this relationship and, consequently, more efforts are needed from both the theoretical and the observational perspectives to improve it.

Weidemann (1977) carried out the first attempt to empirically map this relationship, and provided also a recent revision (Weidemann 2000). Although many improvements have been achieved in these 30 years, there are still some pieces missing in the puzzle. For instance, the dependence of this function on different parameters is still not clear (e.g. metallicity, magnetic field, angular momentum). On the other hand, numerous works have dealt with the calculation of a theoretical initial-final mass relationship (Domínguez et al. 1999; Marigo 2001), but the differences in their evolutionary codes, such as the treatment of convection, the value of the assumed critical mass, which is the maximum mass of a white dwarf progenitor, or the mass loss prescriptions used lead to very different results. The main differences between the different theoretical approaches to the initial-final mass relationship have been extensively discussed in Weidemann (2000).

From an observational perspective, most efforts up to now have focused on the observation of white dwarfs in open clusters, since this allows to infer the total age and the original metallicity of white dwarfs belonging to the clus-

⋆ E-mail: catalan@ieec.uab.es

ter (Williams et al. 2004; Kalirai et al. 2005). Open clusters have made possible the derivation of a semi-empirical initial-final mass relationship using more than 50 white dwarfs, although only covering the initial mass range between 2.5 and 7.0 $M_{\odot}$ because stellar clusters are relatively young and, hence, the white dwarf progenitors in these clusters are generally massive. The recent study of Kalirai et al. (2008) based in old open clusters (NGC 7789, NGC 6819 and NGC6791) has extended this mass range to smaller masses. A parallel attempt to cover the low-mass range of the initial-final mass relationship has been carried out by Catalán et al. (2008). This was the first study of this relationship based in common proper motion pairs. The stars studied in Catalán et al. (2008) are at shorter distances in comparison with star clusters and this allows a better spectroscopic study of both members of the pair, obtaining their stellar parameters with accuracy. At the same time, the study of these pairs enables a wide age and metallicity coverage of the initial-final mass relationship.

The aim of this work is to perform a revision of the initial-final mass relationship taking into account our recent results from studying white dwarfs in common proper motion pairs (Catalán et al. 2008) and the available data that are currently being used to define the initial-final mass relationship. The paper is organized as follows. In §2 we present the analysis of the data that we will use to define the semi-empirical initial-final mass relationship. Section 3 is devoted to the detailed analysis of the semi-empirical initial-final mass relationship derived in this paper and to give some clues on its dependence on some parameters, such as metallicity. In §4 and §5 we compute the luminosity function and the mass distribution of white dwarfs considering different initial-final mass relationships and compare our results with the available observational data. Finally in §6 we summarize our main results and we draw our conclusions.

2 ANALYSIS OF CURRENT AVAILABLE DATA

2.1 Open clusters and visual binaries

We have carried out a re-analysis of the available data currently used to define the semi-empirical initial-final mass relationship, which is mainly based on white dwarfs in open clusters. We have used the white dwarf atmospheric parameters ($T_{\rm eff}$ and $\log g$) derived by other authors, as well as the ages and metallicities of the clusters reported in the literature. To obtain the final and initial masses we followed the procedure described in Catalán et al. (2008). This procedure consists in deriving the final mass ($M_{\rm f}$) and the cooling time of each white dwarf from the atmospheric parameters and the cooling sequences of Salaris et al. (2000). These cooling tracks consider a carbon-oxygen (CO) core white dwarf (with a larger abundance of O at the centre of the core) with a H thick envelope ontop of a He buffer, $q({\rm H}) = M_{\rm H}/M = 10^{-4}$ and $q({\rm He}) = M_{\rm He}/M = 10^{-2}$. As it will be shown in the next section, the thicknesses of these envelops are very important in the cooling of white dwarfs. These improved cooling sequences include an accurate treatment of the crystallization process of the CO core, including phase separation upon crystallization, together with up-to-date input physics suitable for computing white dwarf evolution. Since we know the total ages of these white dwarfs (from the age of the cluster) we derived the main-sequence lifetimes of the progenitors, and from these, their initial masses using the stellar tracks of Domínguez et al. (1999). At present, the atmospheric parameters of white dwarfs can be determined with accuracy if they correspond to the DA type, that is, if their spectra shows uniquely the hydrogen absorption lines. For this reason, and in order to keep consistency in the cooling sequences used we only consider DA white dwarfs in our study. In Table 1 we give the initial and final masses that we have recalculated for white dwarfs in open clusters. Other information such as the atmospheric parameters, cooling times, main-sequence lifetimes of the progenitors and metallicities are also given. Those white dwarfs for which we have obtained a cooling time longer than its total age have not been included in our study, since this is a good indication that the star does not belong to the cluster, or it has not a CO core. To compute the errors of the final masses we have taken into account the errors of the atmospheric parameters. In the case of the initial masses we have taken into account the errors of the cooling times, which come from the atmospheric parameters, and the errors of the total ages of the white dwarfs. When no error for the total age was given in the literature, a value of 10 per cent was adopted. Finally, as reported in Catalán et al. (2008), to derive the initial masses of white dwarfs belonging to common proper motion pairs, the error of the metallicity was also taken into account.

NGC 2099 (M37)

Kalirai et al. (2005) performed spectroscopic observations of 30 white dwarfs belonging to NGC 2099 (M37). Kalirai et al. (2001) determined the age and metallicity of M37, 650 Myr and $Z = 0.011$, respectively. We assume an error of 10 per cent in the age of M37.

NGC 2168 (M35)

We use the atmospheric parameters reported by Williams, Bolte & Koester (2004). Barrado y Navascués et al. (2001) estimated the metallicity of this cluster, [Fe/H]$= -0.21 \pm 0.10$. Thus, we use the stellar tracks corresponding to $Z = 0.012$. As in Williams et al. (2004) we use the age derived by von Hippel (2005), 150 ± 60 Myr. The atmospheric parameters of LAWDS1 and LAWDS27 correspond to new data from Ferrario et al. (2005).

NGC 3532

The cluster data are from Koester & Reimers (1993), although we have used the latest results of Koester & Reimers (1996) reported in Ferrario et al. (2005). According to Ferrario et al. (2005) the age of this cluster is 300 ± 150, and the metallicity is [Fe/H]$= -0.022$ (Twarog, Ashman & Anthony-Twarog, 1997) or [Fe/H]$= -0.02$ (Chen, Hou & Hang, 2003), so we have used the tracks corresponding to $Z = 0.019$. We have also included the data for three white dwarfs reported in Reimers & Koester (1989), although the resolution is a bit lower.

Table 1. Results from re-evaluating the available data.

WD	$T_{\rm eff}$ (K)	$\log g$ (dex)	$M_{\rm f}$ ($M_\odot$)	$t_{\rm cool}$ (Gyr)	$t_{\rm prog}$ (Gyr)	$M_{\rm i}$ ($M_\odot$)	Z
NGC 2099 (M37)							0.011
WD2	19900±900	8.11±0.16	0.69±0.07	0.093±0.019	0.56±0.07	$2.72^{+0.12}_{-0.10}$	
WD3	18300±900	8.23±0.21	0.76±0.09	0.152±0.034	0.50±0.07	$2.82^{+0.16}_{-0.13}$	
WD4	16900±1100	8.40±0.26	0.86±0.12	0.259±0.072	0.39±0.10	$3.06^{+0.32}_{-0.22}$	
WD5	18300±1000	8.33±0.22	0.82±0.11	0.192±0.078	0.46±0.10	$2.90^{+0.26}_{-0.19}$	
WD7	17800±1400	8.42±0.32	0.88±0.14	0.219±0.082	0.43±0.10	$2.96^{+0.30}_{-0.21}$	
WD9	15300±400	8.00±0.08	0.61±0.03	0.182±0.015	0.47±0.07	$2.88^{+0.16}_{-0.13}$	
WD10	19300±400	8.20±0.07	0.74±0.03	0.120±0.010	0.53±0.06	$2.76^{+0.13}_{-0.11}$	
WD11	23000±600	8.54±0.10	0.98±0.04	0.136±0.014	0.51±0.07	$2.80^{+0.13}_{-0.11}$	
WD12	13300±1000	7.91±0.12	0.56±0.05	0.239±0.043	0.41±0.08	$3.01^{+0.23}_{-0.17}$	
WD13	18200±400	8.27±0.08	0.78±0.03	0.167±0.016	0.48±0.07	$2.86^{+0.15}_{-0.12}$	
WD14	11400±200	7.73±0.16	0.45±0.07	0.282±0.039	0.37±0.07	$3.12^{+0.26}_{-0.19}$	
WD16	13100±500	8.34±0.10	0.82±0.05	0.480±0.062	0.17±0.09	$4.10^{+1.44}_{-0.57}$	
NGC 2168 (M35)							0.012
LAWDS 1	32400±512	8.40±0.12	0.89±0.06	0.023±0.006	0.127±0.060	$4.61^{+1.36}_{-0.64}$	
LAWDS 2	32700±603	8.34±0.08	0.85±0.04	0.017±0.003	0.133±0.060	$4.53^{+1.21}_{-0.60}$	
LAWDS 5	52600±1160	8.24±0.09	0.82±0.04	0.0022±0.0001	0.148±0.060	$4.35^{+0.98}_{-0.52}$	
LAWDS 6	55200±897	8.28±0.06	0.84±0.03	0.0020±0.0001	0.148±0.060	$4.35^{+0.98}_{-0.52}$	
LAWDS 15	29900±318	8.48±0.06	0.94±0.03	0.046±0.005	0.104±0.060	$4.99^{+2.25}_{-0.81}$	
LAWDS 22	54400±1203	8.04±0.12	0.72±0.04	0.0025±0.0002	0.147±0.060	$4.35^{+0.98}_{-0.52}$	
LAWDS 27	30500±397	8.52±0.06	0.98±0.03	0.048±0.004	0.102±0.060	$5.03^{+2.37}_{-0.83}$	
NGC 3532							0.019
3532-WD1	28000±2000	8.45±0.45	0.92±0.20	0.055±0.036	0.245±0.154	$3.70^{+1.65}_{-0.55}$	
3532-WD5	28500±2000	7.8±0.3	0.55±0.11	0.013±0.002	0.287±0.150	$3.52^{+1.05}_{-0.46}$	
3532-WD6	28500±3000	8.5±0.5	0.96±0.23	0.060±0.046	0.240±0.157	$3.73^{+1.80}_{-0.57}$	
3532-WD8	23367±1065	7.71±0.15	0.48±0.05	0.023±0.003	0.277±0.150	$3.56^{+1.14}_{-0.48}$	
3532-WD9	29800±616	7.83±0.23	0.56±0.08	0.012±0.001	0.288±0.150	$3.51^{+1.03}_{-0.46}$	
3532-WD10	19267±974	8.14±0.27	0.71±0.11	0.112±0.030	0.188±0.153	$4.05^{+3.53}_{-0.73}$	
Praesepe							0.027
WD0836+201	16629±350	8.01±0.05	0.62±0.02	0.144±0.009	0.481±0.051	$2.97^{+0.11}_{-0.10}$	
WD0836+199	14060±630	8.34±0.06	0.82±0.03	0.39±0.04	0.235±0.064	$3.76^{+0.45}_{-0.28}$	
WD0837+199	17098±350	8.32±0.05	0.81±0.03	0.22±0.02	0.405±0.054	$3.15^{+0.15}_{-0.13}$	
WD0840+200	14178±350	8.23±0.05	0.75±0.02	0.31±0.02	0.315±0.054	$3.42^{+0.21}_{-0.17}$	
WD0836+197	21949±350	8.45±0.05	0.91±0.03	0.13±0.01	0.495±0.051	$2.94^{+0.11}_{-0.09}$	
WD0837+185	14748±400	8.24±0.055	0.76±0.02	0.288±0.018	0.337±0.053	$3.35^{+0.20}_{-0.16}$	
WD0837+218	16833±254	8.39±0.03	0.85±0.01	0.251±0.009	0.374±0.051	$3.23^{+0.16}_{-0.13}$	
WD0833+194	14999±233	8.18±0.035	0.72±0.01	0.246±0.009	0.379±0.051	$3.22^{+0.16}_{-0.13}$	
WD0840+190	14765±270	8.21±0.03	0.74±0.01	0.27±0.01	0.355±0.051	$3.29^{+0.17}_{-0.14}$	
WD0840+205	14527±282	8.24±0.04	0.76±0.02	0.30±0.015	0.325±0.052	$3.39^{+0.20}_{-0.16}$	
WD0843+184	14498±202	8.22±0.04	0.75±0.02	0.295±0.012	0.330±0.051	$3.35^{+0.19}_{-0.15}$	
Hyades							0.027
WD0352+098	14770±350	8.16±0.05	0.71±0.02	0.25±0.01	0.375±0.051	$3.23^{+0.16}_{-0.13}$	
WD0406+169	15180±350	8.30±0.05	0.79±0.02	0.29±0.02	0.335±0.054	$3.35^{+0.20}_{-0.16}$	
WD0421+162	19570±350	8.09±0.05	0.68±0.02	0.096±0.006	0.529±0.050	$2.88^{+0.10}_{-0.09}$	
WD0425+168	24420±350	8.11±0.05	0.70±0.02	0.038±0.003	0.587±0.050	$2.78^{+0.09}_{-0.08}$	
WD0431+125	21340±350	8.04±0.05	0.65±0.02	0.060±0.004	0.565±0.050	$2.82^{+0.09}_{-0.08}$	
WD0438+108	27390±350	8.07±0.05	0.68±0.02	0.018±0.001	0.607±0.050	$2.75^{+0.08}_{-0.08}$	
WD0437+138	15335±350	8.26±0.05	0.77±0.02	0.26±0.01	0.365±0.051	$3.26^{+0.17}_{-0.14}$	

Table 1. Results from re-evaluating the available data (continued). White dwarfs in common proper motion pairs are listed in the last section of this table (CPMPs)

WD	$T_{\rm eff}$ (K)	$\log g$ (dex)	$M_{\rm f}$ ($M_\odot$)	$t_{\rm cool}$ (Gyr)	$t_{\rm prog}$ (Gyr)	$M_{\rm i}$ ($M_\odot$)	Z
NGC 2516							0.02
2516-WD1	28170±310	8.48±0.17	0.95±0.08	0.060±0.012	0.081±0.012	$5.54^{+0.39}_{-0.29}$	
2516-WD2	34200±610	8.60±0.11	1.01±0.04	0.035±0.008	0.106±0.008	$5.03^{+0.14}_{-0.13}$	
2516-WD3	26870±330	8.55±0.07	0.99±0.03	0.082±0.005	0.059±0.005	$6.44^{+0.32}_{-0.29}$	
2516-WD5	30760±420	8.70±0.12	1.07±0.05	0.074±0.014	0.067±0.014	$6.01^{+0.69}_{-0.46}$	
NGC 6791							0.040
WD7	14800±300	7.91±0.06	0.56±0.02	0.17±0.01	8.33±0.85	$1.086^{+0.045}_{-0.038}$	
WD8	18200±300	7.73±0.06	0.47±0.02	0.063±0.005	8.437±0.850	$1.081^{+0.044}_{-0.037}$	
NGC 7789							0.014
WD5	31200±200	7.90±0.05	0.60±0.02	0.010±0.0002	1.39±0.14	$1.84^{+0.07}_{-0.05}$	
WD8	24300±400	8.00±0.07	0.63±0.03	0.029±0.003	1.37±0.14	$1.85^{+0.07}_{-0.05}$	
WD9	20900±700	7.84±0.12	0.54±0.04	0.042±0.006	1.36±0.14	$1.86^{+0.08}_{-0.05}$	
NGC 6819							0.017
WD6	21100±300	7.83±0.04	0.54±0.02	0.041±0.002	2.46±0.25	$1.57^{+0.05}_{-0.05}$	
WD7	16000±200	7.91±0.04	0.57±0.01	0.139±0.005	2.36±0.25	$1.59^{+0.06}_{-0.05}$	
Pleiades							0.019
WD0349+247	32841±172	8.63±0.04	1.03±0.02	0.048±0.004	0.071±0.008	$5.87^{+0.31}_{-0.24}$	
Sirius B	25000±200	8.60±0.04	1.0±0.01	0.108±0.003	0.129±0.012	$4.67^{+0.18}_{-0.16}$	0.020
CPMPs							
WD0315−011	7520±260	8.01±0.45	0.60±0.20	1.20±0.56	$2.97^{+3.09}_{-2.12}$	$1.48^{+0.87}_{-0.28}$	0.016±0.003
WD0413−077	16570±350	7.86±0.05	0.54±0.02	0.112±0.008	0.96±0.37	$2.07^{+0.53}_{-0.27}$	0.008±0.001
WD1354+340	13650±420	7.80±0.15	0.50±0.04	0.20±0.02	$3.06^{+0.74}_{-1.46}$	$1.46^{+0.31}_{-0.09}$	0.015±0.002
WD1544−377	10600±250	8.29±0.05	0.78±0.02	0.76±0.05	0.18±0.50	$4.13^{+?}_{-1.49}$	0.021±0.003
WD1620−391	24900±130	7.99±0.03	0.63±0.01	0.026±0.001	0.30±0.12	$3.45^{+0.65}_{-0.35}$	0.020±0.003
WD1659−531	14510±250	8.08±0.03	0.66±0.01	0.24±0.01	$2.27^{+0.34}_{-0.32}$	$1.58^{+0.08}_{-0.05}$	0.019±0.004

Hyades and Praesepe

We have used the data of Claver et al. (2001) for the Hyades and part of the Praesepe sample. We have included also two stars studied by Dobbie et al. (2004) and some recent results on six new stars (Dobbie et al. 2006). According to von Hippel (2005), the Hyades cluster has an age of 625±50 Myr. We assume the same value for Praesepe, since both belong to the same Hyades supercluster. The metallicity is [Fe/H]= 0.13 according to Chen et al. (2003), so we used the stellar tracks corresponding to $Z = 0.027$.

NGC 2516

We consider the atmospheric parameters derived by Koester & Reimers (1996). The age of the cluster is that determined by Meynet, Mermilliod & Maeder (1993), 141±2 Myr. This cluster has a solar metallicity according to Jeffries, James & Thurston (1998).

NGC 6791, NGC 7789 and NGC 6819

We include the recent results obtained by Kalirai et al. (2008) based on spectroscopic observations of white dwarfs in different old clusters. These results, as well as the ones obtained by Catalán et al. (2008) are somewhat relevant, since constitute the first constraints on the low-mass end of the initial-final mass relationship. NGC 6791 is one of the oldest and most metal-rich open clusters. According to Kalirai et al. (2007), NGC 6791 has an age of 8.5 Gyr and [Fe/H]= $+0.3 \pm 0.5$. We have used the stellar tracks corresponding to $Z = 0.04$. The white dwarfs of this cluster have relatively low masses ($< 0.47\,M_\odot$), so the majority of white dwarfs belonging to this cluster could have a He core (Kalirai et al. 2007). Although it has been suggested that He-core white dwarfs could be formed also by single-evolution (Kilic, Stanek & Pinsonneault, 2007), we prefer not to take these white dwarfs into account, and only consider the two confirmed cluster members with masses above this value. In this case, we assume an error of 10 per cent in the age of NGC 6791.

The white dwarf population of NGC 7789 and NGC

6819 were also studied recently by Kalirai et al. (2008). According to their results, NGC 7789 has an age of 1.4±0.14 Gyr and a metallicity of $Z = 0.014$, while NGC 6819 has an age of 2.5±0.25 Gyr and $Z = 0.017$.

Pleiades

WD0349+247 is the only known Pleiades white dwarf. We have used the atmospheric parameters derived by Dobbie et al. (2006). The age of the Pleiades is 125±8 Myr according to Rebolo, Martin & Magazzu (1992) and it has a metallicity of [Fe/H]= −0.03 (Chen et al. 2003). We use the stellar tracks corresponding to $Z = 0.019$.

Sirius B

Sirius B is a very well-known DA white dwarf that belongs to a visual binary system. Since the separation between the members of this system is ~ 7 AU it can be assumed that there has not been any significant interaction between them during the AGB phase of the progenitor of the white dwarf member (Liebert et al. 2005a). Thus, it can be considered that Sirius B has evolved as a single star, and therefore it is a good candidate for studying the initial-final mass relationship. In this work, we use the atmospheric parameters determined by Liebert et al. (2005a), an age of 237±12 Myr and solar metallicity.

2.2 Globular clusters

In principle, globular clusters could also be used for improving the initial-final mass relationship since they have some characteristics which are similar to those of open clusters, but we have decided not to include them since the study of white dwarfs in globular clusters still suffers from large uncertainties. Globular clusters contain thousands to millions of stars. However, white dwarfs belonging to them are usually very faint due to their large distances, which difficults obtaining high signal-to-noise spectra. Moreover, since globular clusters usually have crowded fields it is also difficult to isolate each star properly when performing spectroscopic observations. Therefore, the reduction procedure, mainly the background substraction, is also more complicated. Up to now, the white dwarf population of globular clusters has been mainly used to determine their distances and ages (Richer et al. 2004). An important attempt to derive the masses of white dwarfs in globular clusters (NGC 6397 and NGC 6752) was carried out by Moehler et al. (2004). However, due to the low signal-to-noise and resolution of the spectra, they were not able to derive their spectroscopic masses independently and had to use a combination of spectra with photometry. Although they calculated an average mass for the white dwarfs in NGC 6752 we have decided not to include this value in our work. Instead, we prefer to use data of individual white dwarfs rather than a binned value for a cluster, contrary to that done in other works (Williams 2007; Kalirai et al. 2008).

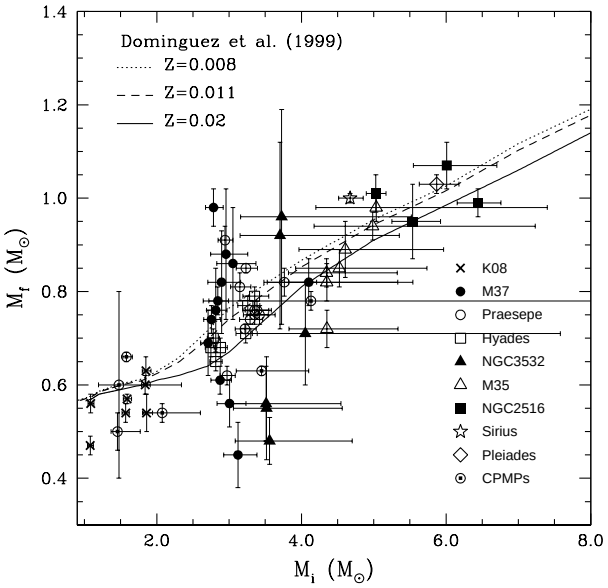


Figure 1. Final masses versus initial masses of the available cluster and common proper motion pairs data.

2.3 Common proper motion pairs

In the case of the common proper motion pairs, the procedure that we followed to derive the final and initial masses of the white dwarfs is explained in detail in Catalán et al. (2008). It mainly consisted in performing independent spectroscopic observations of the components of several common proper motion pairs composed of a DA white dwarf and a FGK star. From the fit of the white dwarf spectra to synthetic models we derived their atmospheric parameters, and from these their masses and cooling times using the cooling sequences of Salaris et al. (2000). In order to derive the initial masses of the white dwarfs we performed independent high-resolution spectroscopic observations of their companions (FGK stars). Since it can be assumed that the members of a common proper motion pair were born simultaneously and with the same chemical composition (Wegner 1973; Oswalt et al. 1988), the ages and metallicities of both members of the pair should be the same. From a detailed analysis of the spectra of the companions we derived their metallicites. Then, we obtained their ages using either stellar isochrones, if the star was moderatly evolved, or the X-ray luminosity if the star was very close to the ZAMS (Ribas et al. in preparation). Once we had the total age of the white dwarfs and the metallicity of their progenitors we derived their initial masses using the stellar tracks of Domínguez et al. (1999). In Table 1 we give the initial and final masses resulting from this study.

3 THE INITIAL-FINAL MASS RELATIONSHIP

In Fig. 1 we present the final versus the initial masses obtained for white dwarfs in common proper motion pairs and open clusters. The observational data that can be used to define the semi-empirical initial-final mass relationship contains now 62 white dwarfs. It is important to emphasize that

all the values below 2.5 $M_{\odot}$ correspond to our data obtained from common proper motion pairs (CPMPs) and the recent data obtained by Kalirai et al. (2008) — K08. Before these studies no data for these small masses were available, since white dwarfs in stellar clusters are usually more massive, especially if the clusters are young. The coverage of the low-mass end of the initial-final mass relationship is specially important since it guarantees, according to the theory of stellar evolution, the study of white dwarfs with masses near the typical values, $M \sim 0.57\,M_{\odot}$, which represent about 90 per cent of the white dwarf population (Kepler et al. 2007). Thus, these new data increase the statistical significance of the semi-empirical initial-final mass relationship.

A first inspection of Fig. 1 reveals that there is a clear dependence of the white dwarf masses on the masses of their progenitors. In Fig. 1, we have also plotted the theoretical initial-final mass relationships of Domínguez et al. (1999) for different metallicities to be consistent with the stellar tracks used to derive the initial masses. Although the distribution presents a large dispersion, a comparison of the observational data with these theoretical relationships shows that they share the same trend. However, it should be noted that for each cluster the data presents an intrinsic spread in mass. The dispersion varies from cluster to cluster, but it is particularly noticeable for the case of M37. Nevertheless, it should be taken into account as well that the observations of M37 were of poorer quality than the rest of the data (Ferrario et al. 2005).

3.1 Main systematic uncertainties

The results obtained are dependent on different assumptions and approaches that we have considered during the procedure followed to derive the final and initial masses, we discuss them separately.

3.1.1 Thicknesses of the H and He envelopes

The fact that the observed white dwarf masses in clusters scatter considerably in the same region of initial masses, as pointed out by other authors — see, for instance, Reid (1996) — may indicate that mass loss could depend more on individual stellar properties than on a global mechanism, and that it could be a stochastic phenomenon, especially on the AGB phase. Mass loss has a large impact on the final composition of the outer layers of white dwarfs, since it defines the thicknesses of the outer He and H (if present) layers. In fact, another reason that may explain why white dwarfs with different final masses could have progenitors with very similar initial masses is the assumption of a given internal composition and outer layer stratification of the white dwarfs under study. The thicknesses of the H and He layers is a key factor in the evolution of white dwarfs, since they control the rate at which white dwarfs cool down. In this work we have used cooling sequences with fixed thicknesses of these envelopes, which might be more appropriate in some cases than in others. In fact, the exact masses that the layers of H and He may have is currently a matter of debate being the subject of several studies. For instance, Prada Moroni & Straniero (2002) computed models reducing the thickness of the H envelope to $q(\mathrm{H}) = 2.32 \times 10^{-6}$, obtaining cooling times shorter than those obtained in this work assuming a thick envelope ($q(\mathrm{H}) = 10^{-4}$). This is natural since H has a larger opacity than He, and H is the major insulating component of the star. In the case of an even thinner H envelope ($q(\mathrm{H}) = 10^{-10}$) the cooling age could be reduced in 10 per cent (1 Gyr) at $\log(L/L_{\odot}) = -5.5$. Thus, the uncertainty in the cooling times could be relevant in some cases, which would affect the estimates of the progenitor lifetimes and in turn, the initial masses derived.

In order to estimate the effect that the thicknesses of H and He envelopes may have in the initial masses derived here, we have repeated the calculations of section 2 but using the cooling sequences of Fontaine, Brassard & Bergeron (2001) for a 50/50 CO core white dwarf with a standard He envelope, $q(\mathrm{He}) = 10^{-2}$, and two different thicknesses for the H envelope, a thick one ($q(\mathrm{H}) = 10^{-4}$) and a thin one ($q(\mathrm{H}) = 10^{-10}$). We have verified that the initial masses are indeed sensitive to the cooling sequences used, as expected. We have obtained larger initial masses when considering a thin envelope, due to the longer cooling times obtained in this case. As previously pointed out, in principle it can be expected that the cooling time scale should be smaller for a thin H envelope model, but this assumption is only true at low enough luminosities (Prada Moroni & Straniero 2002). In fact, at intermediate luminosities a white dwarf with a thinner H envelope evolves slower than the thicker counterpart because it has an excess of energy to irradiate (Tassoul, Fontaine & Winget, 1990). The maximum difference in the initial masses ($\sim 1\ M_{\odot}$) has been found to occur for high-mass progenitors ($M > 5\ M_{\odot}$), while this value is one order of magnitude smaller for smaller masses ($\sim 0.1\ M_{\odot}$). However, it should be noted that many other combinations are possible, for instance, with different thicknesses of the He envelope, which in this case has been kept fixed. However, since it is impossible to know which is the real chemical stratification of the outer layers of each individual white dwarf we have not formally introduced this error in the calculations, since in some cases we would be overestimating the error of the initial masses derived in this work.

3.1.2 Composition of the core

It should be taken into account that besides a CO core, white dwarfs can have other internal compositions. Those white dwarfs more massive than $1.05\ M_{\odot}$ are thought to have a core made of ONe (García-Berro, Ritossa & Iben, 1997; Ritossa, García-Berro & Iben, 1996), while those with masses below $0.4\ M_{\odot}$ have an He-core. ONe white dwarfs cool faster than CO or He white dwarfs because the heat capacity of O and Ne is smaller than that of C or He (Althaus et al. 2007). On the contrary, He white dwarfs are the ones that cool slower (Serenelli et al. 2002). Thus, those white dwarfs studied here with masses near the limits between different populations would be introducing an uncertainty in the cooling times obtained, since their cooling timescales are completely different from one composition to another. For example, a $1\ M_{\odot}$ ONe white dwarf cools 1.5 times faster than a CO white dwarf with the same mass (Althaus et al. 2007). Thus, if an observed white dwarf has indeed a ONe core instead of the typical CO one, its progenitor lifetime would be underestimated in our analysis, and as a consequence, the initial mass derived would be more massive than the real

one. However, the exact impact of this depends also on the total age of the white dwarf. The smaller the total age, the higher the effect of considering a wrong internal composition.

3.1.3 Mass determinations when $T_{\rm eff} \leqslant 12000$ K

The errors reported in our study for the final masses only take into account the errors in the determination of the atmospheric parameters, which can be derived with accuracy if high signal-to-noise spectra are acquired. However, it should be noted that this accuracy decreases considerably at low effective temperatures. According to Bergeron, Wesemael & Fontaine (1992), the atmospheres of DA stars below 12 000 K could be enriched in He while preserving their DA spectral type. This He is thought to be brought to the surface as a consequence of the developement of a H convection zone. Depending on the efficiency of convection the star could still show Balmer lines, instead of being converted into a non-DA white dwarf. Thus, the assumption of an unrealistic chemical composition could have a large impact on the cooling times estimated, but mainly at low effective temperatures. Nevertheless, a very large fraction of the stars in our sample (∼95 per cent) have temperatures well above this limit.

3.1.4 Total age of the white dwarfs

As already pointed out, the derived initial masses depend on the cooling times, the total ages, the metallicity and finally, on the stellar tracks used. Among these parameters the largest source of error is due to the uncertainty in the total ages of the white dwarfs. For white dwarfs in open clusters, the age can be usually derived with high accuracy from model fits to the turn-off location in a colour-magnitude diagram. The uncertainty on the age of a cluster is a systematic effect for stars belonging to the same cluster, since all the initial masses will be shifted together to larger or smaller masses in the final versus initial masses diagram (Williams 2007). On the contrary, in the case of white dwarfs in common proper motion pairs, the accuracy in the total age depends on the evolutionary stage of the companion. The accuracy of the age using isochrone fitting could be high if the star is relatively evolved and located far away from the ZAMS. Using the X-ray luminosity method, described in Catalán et al. (2008), the ages derived could also be quite precise (from 8 to 20 per cent) if the star is relatively young ($t \leqslant 1$ Gyr).

3.2 The semi-empirical relationship

Following closely recent works on this subject (Ferrario et al. 2005; Williams 2007; Kalirai et al. 2008), we assume that the initial-final mass relationship can be described as a linear function. We have performed a weighted least-squares linear fit of the data, obtaining that the best solution is

$$M_{\rm f} = (0.117 \pm 0.004) M_{\rm i} + (0.384 \pm 0.011) \quad (1)$$

where the errors are the standard deviation of the coefficients.

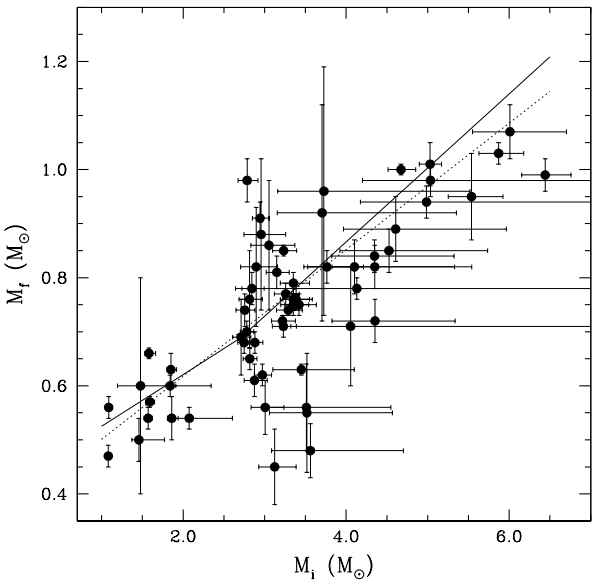


Figure 2. Final masses versus initial masses for the white dwarfs in our sample. Solid and dotted lines correspond to weighted least-squares linear fits of the data.

In Fig. 2 we represent all the data that we have recalculated and this linear fit (dotted line). In past works, since there was not available data in the region of low-mass white dwarfs, a least-squares linear fit led to an unconstrained result (Ferrario et al. 2005). For this reason, a ficticious anchor point at low masses was used to represent the typical white dwarf mass of $M_{\rm f} \sim 0.57\ M_{\odot}$ (Kepler et al. 2007). In our case, this is not necessary since we are now reproducing this well-established peak of the field white dwarf mass distribution thanks to the new data in the low-mass region (Kalirai et al. 2008; Catalán et al. 2008). As can be seen in Fig. 2 the theoretical initial-final mass relationship can be divided in two different linear functions, each one above and below 2.7 $M_{\odot}$, with a shallower slope for small masses probably due to the smaller efficiency of mass loss. Taking this into account we have performed a weighted least-squares linear fit for each region, obtaining

$$M_{\rm f} = (0.096 \pm 0.005) M_{\rm i} + (0.429 \pm 0.015) \quad (2)$$

for $M_{\rm i} < 2.7\ M_{\odot}$, whereas for $M_{\rm i} > 2.7\ M_{\odot}$ we obtain:

$$M_{\rm f} = (0.137 \pm 0.007) M_{\rm i} + (0.318 \pm 0.018) \quad (3)$$

In these expressions the errors are the standard deviation of the coefficients. These two independent fits, which are represented as solid lines in Fig. 2, seem to reproduce better the observational data than a unique linear fit (dotted line). Taking into account the scatter of the data and the values of the reduced χ^2 of these fits (7.1 and 4.4, respectively) we consider that the errors associated to the coefficients are underestimated. A more realistic error can be obtained computing the dispersion of the derived final masses, which is of 0.05 $M_{\odot}$ and 0.12 $M_{\odot}$ respectively. These are the errors that should be associated to the final mass when using the expressions derived here — Eqs. (2) and (3), respectively.

3.3 Dependence on different parameters

As already mentioned in the introduction, there are other parameters besides the mass of the progenitor that may have an impact on the final masses of white dwarfs (e.g. metallicity or rotation). A detailed analysis of the results that we have obtained so far allows us to give some clues on the dependence of the initial-final mass relationship on these parameters. We discuss them below.

3.3.1 Metallicity

The sample of white dwarfs studied here covers a range of metallicities from $Z = 0.006$ to 0.040. From a theoretical point of view it is well established that progenitors with large metallicity produce less massive white dwarfs — see the relations of Domínguez et al. (1999) plotted in Fig. 1. Thus, one should expect to see a dependence of the semi-empirical data on metallicity. Our purpose in this section is to compare data with the same and different metallicity and evaluate if the differences in the derived masses are smaller or greater in this two cases. Open clusters are appropriate for carrying out such comparison, since all the stars belonging to a particular cluster have the same metallicity. For instance, in the case of the two stars from Praesepe (open circles in Fig. 1) with initial masses around 3.0 $M_{\odot}$, the white dwarfs differ in $\Delta M_{\rm f} = 0.3\ M_{\odot}$. However, for the rest of stars in this cluster, the dispersion is significantly smaller (a factor of 2). Thus, the large spread could be explained by considering that may be these objects are field stars. However, the sample of white dwarfs in the Praesepe cluster has been well studied (Claver et al. 2001; Dobbie et al. 2004) and it is unlikely that these stars do not belong to the cluster. The Hyades also contain a large number of white dwarfs, for which the initial and final masses have been derived with accuracy. In this case, all the data points fall in the region limited by the theoretical relations of Domínguez et al. (1999), and the scatter is $\Delta M_{\rm f} = 0.1\ M_{\odot}$, which is the same as the difference between the theoretical relations corresponding to $Z = 0.008$ and $Z = 0.02$. This is the minimum scatter found in the observational data, since the points corresponding to the Hyades, together with those of Praesepe, are the ones with smaller error bars. In any case, this scatter, although smaller than in other cases, is still larger than the uncertainties, which prevents to derive any clear dependence on metallicity. As previously pointed out, the data of M37 present the largest scatter in the sample ($\Delta M_{\rm f} = 0.5\ M_{\odot}$), but it should be noticed that the errors in the final masses are considerably larger than for the rest of the clusters.

It is important to evaluate if the dispersion increases when data with different metallicities is considered. Comparing points with the same initial mass but different metallicities, it can be noted that $\Delta M_{\rm f}$ is of the same order as in the case of equal metallicities. For example, comparing the data of M37 and the data of the Hyades — which have metallicities $Z = 0.011$ and $Z = 0.027$, respectively — for an initial mass around 3 $M_{\odot}$, $\Delta M_{\rm f}$ is $\sim 0.5\ M_{\odot}$, but this scatter is the same when we compare data from M37 only. However, the scatter decreases when we analyse larger initial masses. If the data of M35 and M37 are compared (metallicites $Z = 0.011$) with the data of NGC3532 and one of the common proper motion pairs located at $\sim 4.0\ M_{\odot}$ (with $Z = 0.02$), it can be seen that the maximum $\Delta M_{\rm f}$ is 0.2 $M_{\odot}$, although this is also what we obtain when we compare only the data of M35 located in this region. In the region of small masses we have data ranging from $Z = 0.008$ to $Z = 0.04$, but the maximum scatter is the same regardless of the metallicity of the stars ($\Delta M_{\rm f} = 0.1\ M_{\odot}$). Finally, at the high-mass end we find the same dispersion, although in this case the data have the same metallicity. Thus, considering the current accuracy of the available observational data we do not find any clear dependence of the semi-empirical initial-final mass relationship on metallicity.

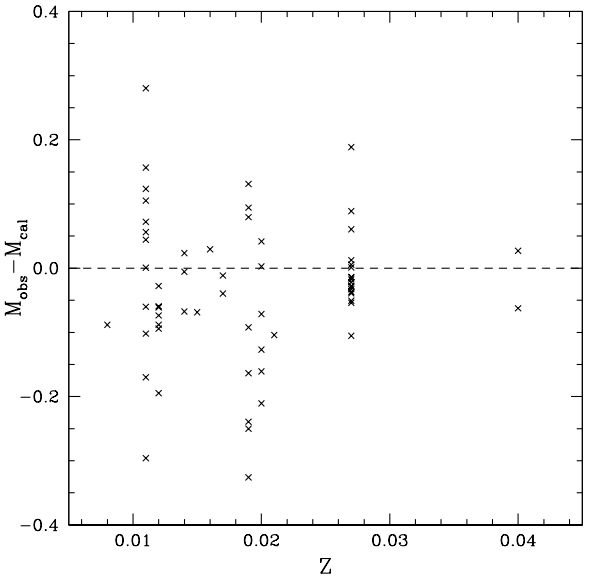


Figure 3. Correlation between final masses and metallicity.

It is interesting to perform a more quantitative study of the correlation between the final masses and metallicity. In Fig. 3 we plot the differences between the observed final masses and the final masses obtained using Eqs. (2) and (3) as a function of metallicity. The dashed line corresponds to the hypothetical case in which there is no difference between the observational and the values predicted by these relations. In order to quantify the correlation in the sample of points presented in Fig. 3, we have calculated the Spearman rank correlation coefficient. The value obtained is 0.036, which is very close to zero, indicating that there is an extremely weak positive correlation between the difference in the final masses and metallicity. Since the Spearman correlation does not take into account the errors of the values considered, we have carried out a bootstrapping in order to evaluate the actual uncertainty on the correlation coefficient without any assumption on the error bars. This consists on choosing at random N objects from our sample (which has also N objects) allowing repetition, and then calculating the new correlation coefficient for each of these new samples. We have performed this a large number of times (5000) obtaining a mean correlation coefficient of -0.002 ± 0.128. Thus, we conclude that the final masses and metallicity of this sample does not present any correlation, and that the scatter in the distribution in Fig. 1 is not due to the effect of metallicity. Of course, it should be taken into account that the observed

final masses have been derived using the atmospheric parameters reported by different authors who have considered also different white dwarf models, although the prescriptions used in the fits are usually those of Bergeron et al. (1992) in all the cases.

It is worth comparing our results with other works. For instance, Kalirai et al. (2005) claimed that they had found the first evidence of a metallicity dependence on the initial-final mass relationship. They noticed that half of their data of M37 (also plotted in Fig. 1) were in agreement with the theoretical relationship of Marigo (2001), and considered this result as an indication of dependence on metallicity. On the other hand, in a recent revision of the semi-empirical initial-final mass relationship, Williams (2007) analyzed part of the cluster data discussed here by deriving a binned semi-empirical initial-final mass relationship. This consisted in associating an initial and a final mass for each cluster by calculating the mean of the initial and final masses of the individual white dwarfs belonging to that cluster. Then, they compared these values as function of metallicity and, as in our case, they did not find a clear dependence of the semi-empirical data on metallicity. In fact, their conclusion was that metallicity should affect the final mass only in 0.05 $M_{\odot}$, considering an initial mass of 3 $M_{\odot}$, which is in good accord with our results.

3.3.2 Rotation

According to Domínguez et al. (1996), fast rotating stars produce more massive white dwarfs than slow rotating stars. The models calculated by Domínguez et al. (1996) including rotation predict that for a fast rotating star with an initial mass of 6.5 $M_{\odot}$ the white dwarf produced has a mass in the range 1.1 to 1.4 $M_{\odot}$, which is considerably larger than when rotation is disregarded (Domínguez et al. 1999). Among our sample of white dwarfs in common proper motion pairs there are two stars (WD1659−531 and WD1620−391) that might exemplify the effect that rotation may have in stellar evolution. The companion of WD1659−531, HD153580, is a fast rotating star according to Reiners & Schmitt (1993), with a tangential velocity $v \sin i = 46 \pm 5$ km s^{-1}. Thus, we can hypotetically assume that the progenitor of WD1659−531 was also a fast rotator. If we compare the masses derived for these stars (Table 1) we can note that starting from an initial mass of 1.58 $M_{\odot}$, which is more than two times smaller than the progenitor of WD1620−391 (3.45 $M_{\odot}$), it ends up as a white dwarf with approximately the same mass, 0.66 $M_{\odot}$. This indicates that the progenitor of WD1659−531 lost less mass during the AGB phase than the progenitor of WD1620−391. These differences may not be related to metallicity, since both progenitors had solar composition. Thus, we think that this could be the first evidence showing that rotation may have a strong impact in the evolution of a star, leading to more massive white dwarfs, as suggested by Domínguez et al. (1996).

3.3.3 Magnetism

One way to detect the presence of magnetic fields in white dwarfs is by performing spectropolarimetric observations. Some of the white dwarfs belonging to this sample have been the subject of studies to investigate their magnetic nature. In particular, WD 0837+199 (also known as EG61), which belongs to Praesepe, is the only known magnetic white dwarf in an open cluster. The magnetic field of this star is of 3 MG according to the study of Kawka et al. (2007). The mass that we have obtained for this star is 0.81 $M_{\odot} \pm 0.03$ $M_{\odot}$ (see Table 1), rather large, although a bit smaller than the typical mass of magnetic white dwarfs, which is around 0.93 $M_{\odot}$ (Wickramasinghe & Ferrario 2005). Regarding white dwarfs in common proper motion pairs, Kawka et al. (2007) also obtained circularly polarized spectra of WD0413−017, WD1544−377, WD1620−391 and WD1659−531, finding evidence of magnetism only for the first of these stars. This result is in good agreement with the findings of other authors (Aznar Cuadrado et al. 2004; Jordan et al. 2007). In the case of WD0413−017, more commonly known as 40 Eri B, the magnetic field is rather weak, 2.3 kG, and the mass that we have derived is 0.54±0.02 $M_{\odot}$. Although the mass of this star is well below the typical mass of magnetic white dwarfs, it is in good agreement with the rest of white dwarfs studied by Kawka et al. (2007) at the kG level. If we do not consider WD 0837+199 and WD0413−017 in the fit carried out in the last section we obtain negligible changes on the expressions derived.

Spectropolarimetric surveys of white dwarfs have suggested that there is a decline in the incidence of magnetism of stars with fields $B < 10^6$ G, although this incidence seems to rise again when the field is much lower, $B < 100$ kG (Wickramasinghe & Ferrario 2005). The sample of white dwarfs that we have considered in this work contains two magnetic white dwarfs, one with a strong magnetic field and the other with a rather weak magnetic field. Although the influence of the magnetic field in stellar evolution has not been yet established, we find that the final masses obtained in these two cases are very different, being larger when the magnetic field is stronger. So, it is reasonable to think that the magnetic field could play a key role on the evolution of the progenitor star. However, with the current data on the magnetic white dwarfs belonging to the sample of white dwarfs used in this work it is not possible to favor one of the two main hypothesis regarding this issue: whether magnetic white dwarfs are more massive because the progenitors were also more massive (without any dependence on the magnetic field), or on the contrary, magnetic white dwarfs are more massive because the magnetic field had an influence during its evolution, favoring the growth of the core.

According to Kawka et al. (2003), 16 per cent of the white dwarf population should be comprised by magnetic white dwarfs. So, among the sample of stars considered in this work, we could expect 9-10 white dwarfs to be magnetic. Thus, spectropolarimetric observations of the current sample of white dwarfs used to define the semi-empirical initial-final mass relationship would be very useful to shed some light upon this subject.

4 THE WHITE DWARF LUMINOSITY FUNCTION

The white dwarf luminosity function is defined as the number of white dwarfs per unit volume and per bolometric magnitude — see, for instance, Isern et al. (1998):

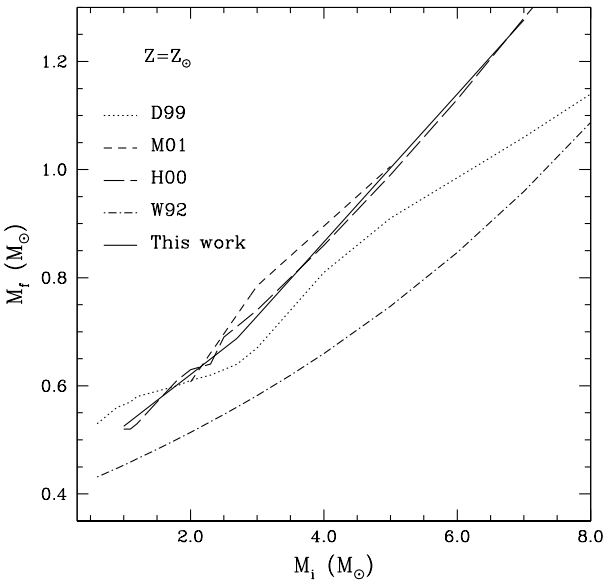


Figure 4. Initial-final mass relationship according to different authors: Domínguez et al. (1999) — D99 — Marigo (2001) — M01 — Hurley et al. (2000) — H00 — Wood (1992) — W92 — and the one derived in this work.

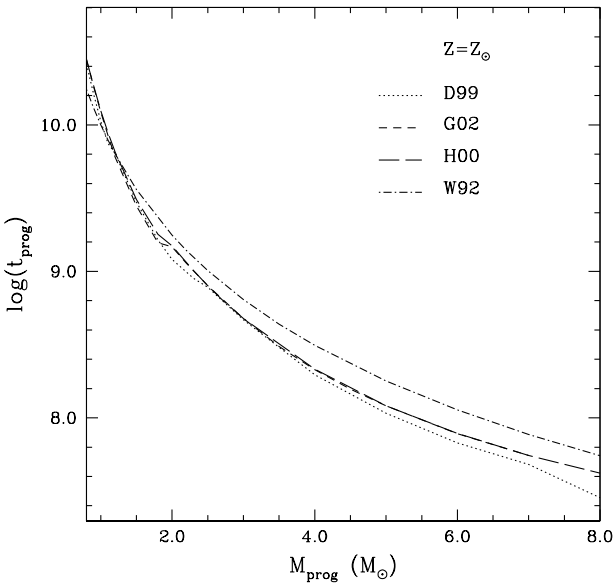


Figure 5. Main sequence lifetime versus stellar mass according to different authors: Domínguez et al. (1999) — D99 — Girardi et al. (2002) — G02 — Hurley et al. (2000) — H00 — and Wood (1992) — W92.

$$n(M_{\rm bol},T)=\int_{M_{\rm i}}^{M_{\rm s}}\phi(M)\psi(T-t_{\rm cool}-t_{\rm prog})\tau_{\rm cool}\,dM \qquad (4)$$

where M is the mass of the progenitor of the white dwarf, $\tau_{\rm cool}=dt/dM_{\rm bol}$ is its characteristic cooling time, $M_{\rm i}$ and $M_{\rm s}$ are the minimum and maximum mass of the progenitor star able to produce a white dwarf with a bolometric magnitude $M_{\rm bol}$ at time T, $t_{\rm cool}$ is the time necessary to cool down to bolometric magnitude $M_{\rm bol}$ — for which we adopt the results of Salaris et al. (2000) and Althaus et al. (2007) for CO and ONe white dwarfs, respectively — $t_{\rm prog}$ is the lifetime of the progenitor, T is the age of the population under study, $\psi(t)$ is the star formation rate — which we assume to be constant — and $\phi(M)$ is the initial mass function, for which we adopt the expression of Salpeter (1955).

4.1 The influence of the progenitors

To compute the white dwarf luminosity function it is also necessary to provide a relationship between the mass of the progenitor and the mass of the resulting white dwarf, that is, the initial-final mass relationship. Additionally, the influence of the progenitors in Eq. (4) appears through the age assigned to the progenitor, which determines the star formation rate, and through the cooling time, $t_{\rm cool}$ and the characteristic cooling time, $\tau_{\rm cool}$, which depend on the mass of the white dwarf. In order to evaluate the influence of these inputs, we have computed a series of theoretical white dwarf luminosity functions using several initial-final mass relationships (Fig. 4) and evolutive tracks for the progenitor stars (Fig. 5). Whenever possible we have adopted the same set of stellar evolutionary inputs, that is, the initial-final mass relationship and the main-sequence lifetime corresponding to the same set of calculations.

We compare the resulting theoretical luminosity functions with the data obtained by averaging the different observational determinations of the white dwarf luminosity function (Knox, Hawkins & Hambly, 1999; Leggett, Ruiz & Bergeron, 1998; Oswalt et al. 1996; Liebert, Dahn & Monet, 1988). The theoretical white dwarf luminosity functions were also normalized to the observational value with the smallest error bars in number density of white dwarfs, that is $\log(N)=-3.610$, $\log(L/L_{\odot})=-2.759$, avoiding in this way the region in which the cooling is dominated by neutrinos (at large luminosities) and the region in which crystallization is the dominant physical process — at luminosities between $\log(L/L_{\odot})\simeq-3$ and -4.

Fig. 6 shows the resulting white dwarf luminosity functions when different stellar evolutionary inputs are used. At low luminosities it can be noticed the characteristic sharp down-turn in the density of white dwarfs. This cut-off in the number counts has been interpreted by different authors (Winget et al. 1987; García-Berro et al. 1988) as the consequence of the finite age of the Galactic disc. Thus, a comparison between the theoretical luminosity functions and the observational data can provide information about the age of the Galactic disc. In this figure the cut-off of the observational white dwarf luminosity function has been fitted using an age of the disc of $T=11$ Gyr for all the cases except for the case in which the expressions of Wood (1992) were used. In this last case the best-fitting is obtained using $T=10.5$ Gyr. This can be understood by comparing the different stellar evolutionary inputs considered in this work. As can be seen in Fig. 4, the initial-final mass relationship of Wood (1992) is the one that produces less massive white dwarfs. The semi-empirical relationship that we have derived in this work is similar to that of Hurley, Pols & Tout (2000). Marigo (2001) predicts more massive white

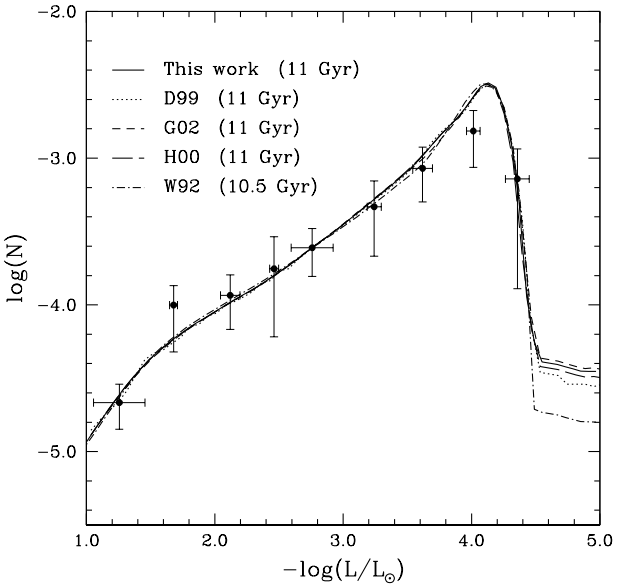


Figure 6. White dwarf luminosity functions considering different evolutive stellar models and initial-final mass relationships: Domínguez et al. (1999) — D99— Girardi et al. (2002) — G02 — Hurley et al. (2000) — H00 — Wood (1992) — W92 — and the relation derived in this work. See text for details.

dwarfs at the intermediate mass domain, whereas the results of Domínguez et al. (1999) produce more massive remnants for the low-mass end and less massive white dwarfs for the high mass end, but always substantially larger than those obtained with the initial-final mass relationship of Wood (1992). These differences mainly arise from the procedure used to calculate each theoretical initial-final mass relationship. The relations derived by Domínguez et al. (1999) and Marigo (2001) are obtained using fully evolutive models but using different treatments of convective boundaries, mixing and mass-loss rates on the AGB phase. On the other hand, the relations of Hurley et al. (2000) were obtained from a fitting of the observational data from eclipsing binaries and open clusters, obtaining analytic formulae for different metallicities. Finally, the relation of Wood (1992) is an exponential expression derived from a fit to the PNN mass distribution. In Fig. 5 we show the different main-sequence lifetimes as a function of the main-sequence mass. In those cases in which there was a dependence on metallicity we have adopted $Z = Z_{\odot}$. As it can be seen there, the behaviour of the different main-sequence lifetimes is very similar, although for the case of Wood (1992), stars spend more time in the main-sequence than in the rest of cases, especially for those stars with large masses. Considering this, one should expect that the fit of the cut-off of the white dwarf luminosity function would correspond to a longer Galactic disc age when using the expressions of Wood (1992). On the contrary, we have obtained a younger Galactic disc. The longer progenitors lifetimes of Wood (1992) are in part compensated by the fact that its corresponding initial-final mass relationship favors the production of low-mass white dwarfs, which cool down faster at high luminosities. A simple test can be done by using, for example, the stellar tracks of Domínguez et al. (1999), which give shorter progenitor lifetimes, and the initial-final mass relationship of Wood (1992). In this case we obtain a Galactic disc age of 10 Gyr, 1 Gyr younger than if we consider any of the other initial-final mass relationships shown in Fig. 4. Thus, the behaviour of the relation of Wood (1992) is clearly different from others in the literature, and this has important implications on the resulting white dwarf luminosity functions.

Comparing the results of Fig. 6 it can be noticed that for the hot end of the white dwarf luminosity function there are not differences whatsoever. In fact, all the theoretical luminosity functions are remarkably coincident. The only visible differences, although not very relevant, occur just after the crystallization phase has started, at $\log(L/L_{\odot}) \simeq -4.0$. Two essential physical processes are associated with crystallization, namely, a release of latent heat and a modification of the chemical concentrations in the solid phase. Both provide extra energy sources and lengthen the cooling time of the star. This is the reason why all the theoretical calculations predict a larger number of white dwarfs for these luminosity bins. Beyond the cut-off, we find that the density of white dwarfs is smaller in the case of Wood (1992), and this is because this region is dominated by massive white dwarfs, since the progenitors of these stars were also massive, and as shown in Fig. 5 spent less time at the main-sequence. Thus, massive white dwarfs have had enough time to cool down to such low luminosities. In any case, it is worth mentioning that low-mass white dwarfs cool faster at high luminosities, but for small luminosities it occurs just the opposite, since massive white dwarfs crystallize at larger luminosities, and this implies smaller time delays.

4.2 The luminosity function of massive white dwarfs

4.2.1 Effect of the initial-final mass relationship

The influence of the initial-final mass relationship on the white dwarf luminosity function should be more evident when it is constrained to massive white dwarfs (Díaz-Pinto et al. 1994). Recently, Liebert, Bergeron & Holberg (2005b) performed high signal-to-noise spectroscopic observations of more than 300 white dwarfs belonging to the Palomar Green (PG) Survey. The analysis of this set of data has provided us with a sample of white dwarfs with well determined masses that allows for the first time the study of the white dwarf luminosity function of massive white dwarfs (Isern et al. 2007). Unfortunately, according to Liebert et al. (2005b) the completeness of the sample decreases severely near 10 000 K, where white dwarfs with small masses (0.4 $M_{\odot}$) are brighter ($M_{\rm V} \sim 11$) than massive white dwarfs with $M > 0.8\ M_{\odot}$ (which have visual magnitudes around $M_{\rm V} \sim 13$). Consequently, above $M_{\rm V} = 11$ this survey only has detected white dwarfs with masses larger than 0.4 $M_{\odot}$. Therefore, we will limit the analysis to white dwarfs brighter than $M_{\rm V} \sim 11$.

We have computed a set of white dwarf luminosity functions considering an age of 11 Gyr for the Galactic disc and using bins of visual magnitude. In Fig. 7 we show from top to bottom the total luminosity function and the luminosity functions of white dwarfs with masses larger than 0.7 $M_{\odot}$ and 1.0 $M_{\odot}$, respectively. The total luminosity func-

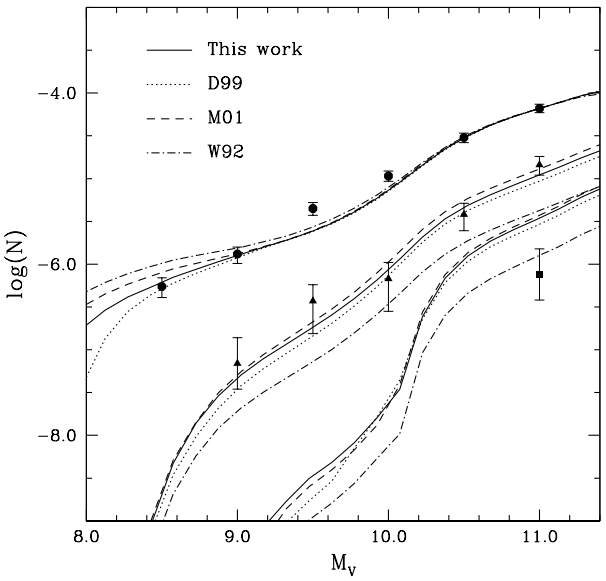


Figure 7. White dwarf luminosity functions versus visual magnitude using different initial-final mass relationships: Domínguez et al. (1999) — D99 — Marigo (2001) — M01 — Wood (1992) — W92 — and this work. From top to bottom we show the total luminosity function, and the luminosity functions of white dwarfs with masses larger than 0.7 $M_{\odot}$ and 1.0 $M_{\odot}$. Circles, triangles and squares correspond to the observational data of Liebert et al. (2005b).

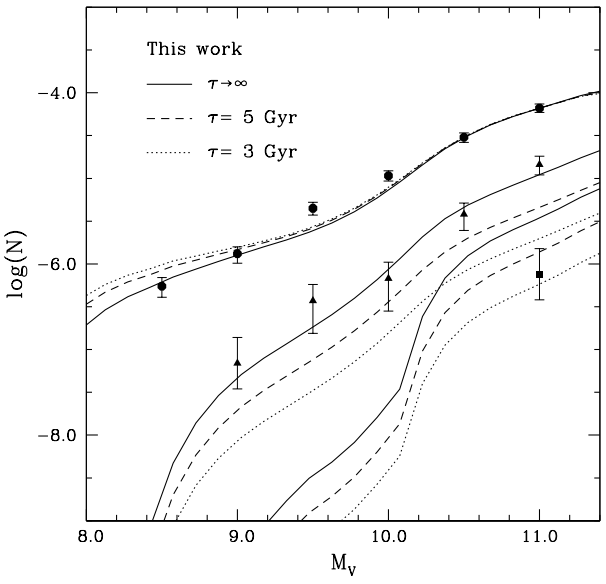


Figure 8. White dwarf luminosity functions versus visual magnitude using the initial-final mass relationship derived in this work and different star formation rates. Circles, triangles and squares correspond to the observational data of Liebert et al. (2005b).

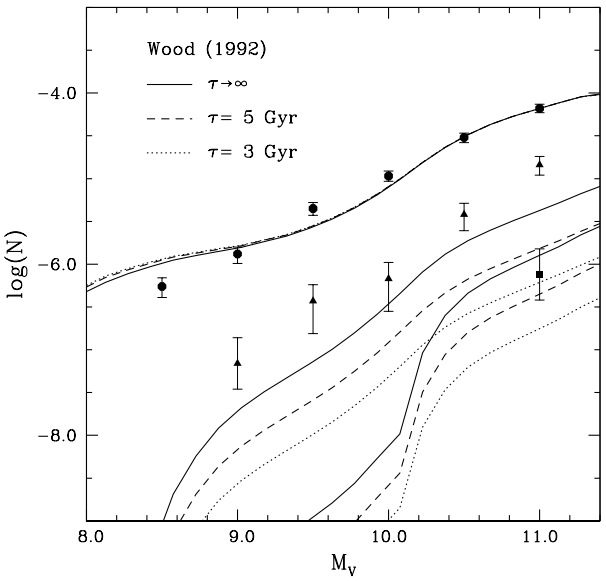


Figure 9. Same as Fig. 8 but using the initial-final mass relationship of Wood (1992).

tion (that is, considering the whole the range of masses) was normalized to the bin corresponding to $M_{\rm V} = 11$, and then, this normalization factor was used for the luminosity functions of white dwarfs more massive than 0.7 $M_{\odot}$ and 1.0 $M_{\odot}$. In this case, we have used the stellar evolutionary inputs of Domínguez et al. (1999), Marigo (2001), Wood (1992) and the semi-empirical initial-final mass relationship that we have derived in the previous section. Comparing the different theoretical luminosity functions, it can be noted that the predicted number of massive white dwarfs is larger when using the inputs of Domínguez et al. (1999), Marigo (2001) and our semi-empirical initial-final mass relationship in comparison with the results obtained when considering the expressions of Wood (1992). This is obviously due to the fact that the initial-final mass relationship of Wood (1992) favors the production of low-mass white dwarfs. It can also be noted that the density of massive white dwarfs is slightly larger when considering the initial-final mass relationship of Marigo (2001) than that obtained when using the initial-final mass relationship derived here. The reverse is true when the initial-final mass relationship of Domínguez et al. (1999) is used. Without considering the results obtained when the expressions of Wood (1992) are used, it can be noted that it is not possible to evaluate which initial-final mass relationship produces a theoretical luminosity function that better fits the observational data, since the error bars of the observational data are larger than the differences between the theoretical results. In any case, what it can be clearly seen is that all the theoretical relations predict more massive white dwarfs than the observations when a mass cut of 1.0 $M_{\odot}$ is adopted, except in the case of Wood (1992).

4.2.2 Effect of the star formation rate

The star formation rate considered in our calculations has also an important influence on the number of massive white

dwarfs produced. In our previous calculations we have considered a constant star formation rate, which has led us to obtain more massive white dwarfs than those detected in the PG Survey. To evaluate the effect of the star formation rate on the white dwarf luminosity function we have repeated the calculations considering the semi-empirical initial-final mass relationship derived in this work and an exponentially decreasing star formation rate $\psi(t) = \exp(-t/\tau)$, with $\tau = 3$ and 5 Gyr, respectively. As it can be noted from Fig. 8 the production of massive stars decreases considerably when a exponentially decreasing star formation rate is considered. The observational data corresponding to the whole range of white dwarf masses and to masses larger than 0.7 $M_{\odot}$ is better fitted when a constant star formation rate ($\tau \rightarrow \infty$) is assumed in the theoretical calculations. On the contrary, for white dwarfs with masses larger than 1.0 $M_{\odot}$ the agreement is better if we consider a variable star formation rate. However, for such massive stars there is only data for one magnitude bin. More observations corresponding to massive white dwarfs are needed to confirm this behaviour of the luminosity function.

For the sake of comparison we have carried out the same calculations but considering the expressions of Wood (1992). The resulting luminosity functions are shown in Fig. 9. In this case, the observational data for stars with masses larger than 0.7 $M_{\odot}$ is not fitted regardless of the star formation rate assumed. On the contrary, the fit is better when considering stars with masses above 1.0 $M_{\odot}$. Since there are more observational data for the range of masses above 0.7 $M_{\odot}$, we find more reliable the conclusions that can be obtained from a comparison of these data than those obtained from only one magnitude bin, as is the case of more massive white dwarfs. Thus, it seems clear that observations rule out the initial-final mass relationship of Wood (1992), and that the other initial-final mass relationships used in this work seem to be more reliable, although the present status of the observational data does not allow to draw a definite conclusion about which initial-final mass relationship is more adequate.

5 THE WHITE DWARF MASS DISTRIBUTION

The understanding of the precise shape of the mass distribution of white dwarfs offers a sorely needed insight about the total amount of mass lost during the course of the last phases of stellar evolution. Thus, a detailed study of this function, from both the theoretical and the observational perspectives can give us clues on the initial-final mass relationship (Ferrario et al. 2005). For that purpose, we have computed a series of theoretical mass distributions using different evolutive stellar models and their corresponding initial-final mass relationships, if available. As in the case of the white dwarf luminosity function we have adopted an age of 11 Gyr for the Galactic disc, a constant star formation rate and the initial mass function of Salpeter. The theoretical mass distributions were then normalized to unit area.

Our purpose is to compare our results with the observational data obtained by Liebert et al. (2005b) from the PG Survey — left panel of Fig. 10 — and the recent data obtained by DeGennaro et al. (2008) from the SDSS — right panel of Fig. 10. As previously pointed out, the accuracy on the mass determinations decreases considerable when white dwarfs are cooler than 12 000 K. Hence, both the theoretical and the observational mass distributions in this section consider white dwarfs with $T_{\rm eff} \geqslant 12\,000$. In the case of the data from the PG Survey, we have computed the observational mass distribution considering the $V_{\rm max}$ values reported by (Liebert et al. 2005b) taking into account the errors in the masses assuming a gaussian distribution. Then, the final distribution has been normalized to unit area, as it was done when considering the theoretical mass distributions. In the case of the data from the SDSS, the observational data shown in Fig. 10 (right) is the mass distribution computed by DeGennaro et al. (2008).

In Fig. 10 we plot our results considering the stellar evolutionary inputs of Domínguez et al. (1999), Girardi et al. (2002) and Wood (1992). We also show our results when considering the evolutive stellar models of Domínguez et al. (1999) and the initial-final mass relation derived in this work, as well as the relation recently obtained by Kalirai et al. (2008). All the white dwarf distributions have been normalized to the total density obtained in each case. As it can be noted, there is a well defined peak in all the mass distributions, the location of which is defined mainly by the initial-final mass relationship considered. On the contrary, the height of the peak depends also on the lifetime of the progenitors. This can be understood with the help of Fig. 4. The most abundant stars are those with small masses (~ 1 $M_{\odot}$). In the case of Wood (1992) and Girardi et al. (2002), the white dwarfs corresponding to these progenitors have masses well below ~ 0.6 $M_{\odot}$, and this is the reason why the central peak is located at smaller masses in Fig. 10. This peak is then shifted to larger masses when the initial-final mass relationship considered favors the production of more massive white dwarfs for the low mass progenitors. This is the case of the semi-empirical initial-final mass relationship of Kalirai et al. (2008), our relationship or the theoretical relation of Domínguez et al. (1999). Note that in the latter case, the production of massive white dwarfs is not favored, opposite to what occurs to our semi-empirical relationship, but the peak is located at the same mass since low-mass progenitors are the ones that dominate.

If we compare the theoretical mass functions with the observational data of Liebert et al. (2005b) from the PG Survey (left panel of Fig. 10) and the recent data obtained by DeGennaro et al. (2008) from the SDSS (right panel of Fig. 10) it can be noted how in both cases the location of the central peak is well fitted by the predictions corresponding to our semi-empirical relationship and the theoretical relation of Domínguez et al. (1999). The height of the peak is better fitted when considering our semi-empirical relationship, although a bit lower in comparison with the SDSS data. The sample of white dwarfs corresponding to the SDSS is very complete since it includes the 1733 stars with $g \leqslant 19$ and $T_{\rm eff} \geqslant 12\,000$ K present in the SDSS DR4, which is seven times the population covered by the PG Survey.

It is worth mentioning that we have not included the He white dwarf population in our calculations. This is the reason why there are no white dwarfs below a certain mass threshold (0.45 $M_{\odot}$ in the case of our semi-empirical initial-final mass relationship). The observational data (both from the PG survey or the SDSS) do indeed present a certain number of white dwarfs in this low-mass region. On the

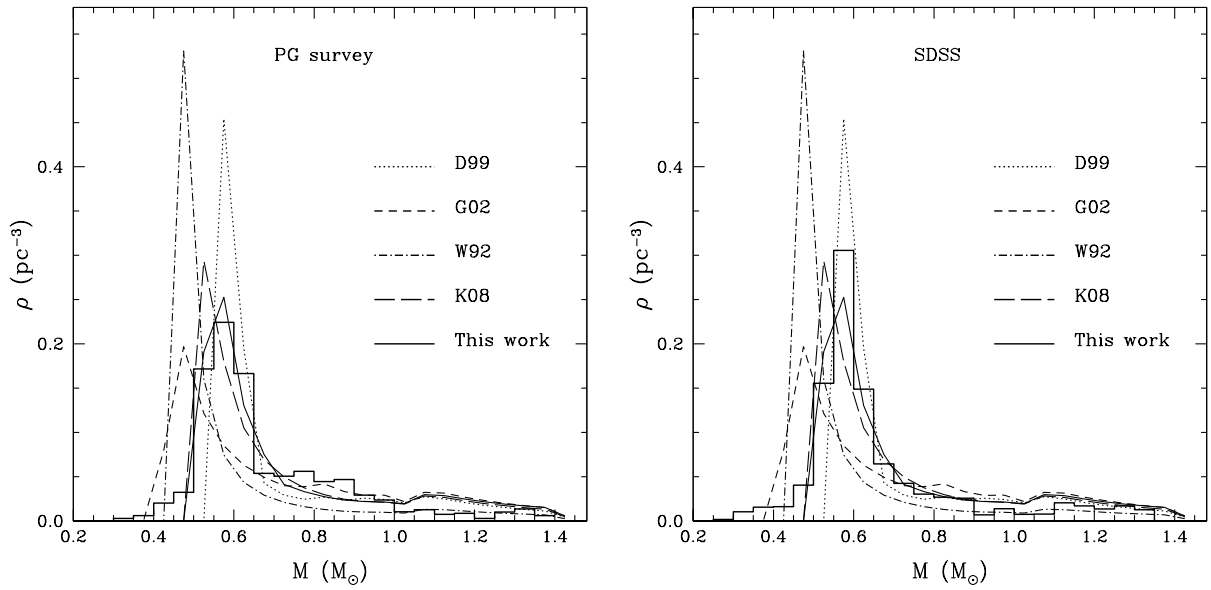


Figure 10. Mass distributions for white dwarfs with $T_{\rm eff} \geqslant 12\,000$ K considering different evolutive stellar models and initial-final mass relationships: Domínguez et al. (1999) — D99 — Girardi et al. (2002) — G02 — Wood (1992) — W92 — Kalirai et al. (2008) — K08 — and the relation derived in this work. The histogram represents the results obtained by Liebert et al. (2005b) corresponding to the data collected in the PG Survey (left) and those obtained by DeGennaro et al. (2008) corresponding to the data in the SDSS (right).

other hand, we have included the ONe white dwarf population which is thought to be dominant for masses larger than 1.05 $M_{\odot}$. ONe-core white dwarfs cool faster than CO-core white dwarfs due to the large heat capacity of C in comparison with that of O and Ne. For this reason a bump located at 1.05 $M_{\odot}$ in the mass distribution that corresponds to the change of the cooling rate is clearly visible. Since the cooling rate is larger for the ONe white dwarf population, there is an increase of the number of white dwarfs produced in this region. As it can be noted in Fig. 10 the density of massive white dwarfs is remarkably lower when considering the initial-final mass relationship of Wood (1992) since it predicts less massive white dwarfs. In the rest of cases the white dwarf mass distributions are approximately coincident in this region.

6 SUMMARY AND CONCLUSIONS

In this work we have revisited the initial-final mass relationship and discussed it in a comprehensive manner. With this purpose, we have re-evaluated the available data in the literature, mainly based on open clusters, that are currently being used to define the semi-empirical initial-final mass relationship. We have used the atmospheric parameters, total ages and metallicities reported in the literature and followed the procedure described in Catalán et al. (2008) to derive the initial and final masses of these white dwarfs. Thanks to these data and our own work based on common proper motion pairs we have been able to collect a very heterogeneous sample of white dwarfs, covering a wide range of ages and metallicites. Most importantly, with this study we have covered the range of initial masses from 1 to 6.5 $M_{\odot}$, which was poorly covered until recently (Kalirai et al. 2008; Catalán et al. 2008). The extension of the initial-final mass relationship to the low-mass end is important since we are now studying the most populated region of initial masses according to the initial mass function of Salpeter, and this means that we are also reproducing the well-established peak of the field white dwarf mass distribution (Kepler et al. 2007).

As discussed previously, for each cluster the results present an intrinsic mass spread, which may indicate that mass loss could depend more on individual stellar properties than on a global mechanism. Thus, mass-loss processes could even be a stochastic phenomenon (Reid 1996), being thus impossible to reproduce with models. Another explanation for the spread of masses found for each cluster could lie on the fact that we do not know the internal composition of the white dwarfs in our sample, and we are using cooling sequences that have fixed values for the C/O ratio at the core and most importantly, fixed thicknesses of the H and He envelopes which may not be appropriate to describe the cooling of individual white dwarfs in some cases. This fact could affect the cooling times derived in approximately 10 per cent at very low luminosities (Prada Moroni & Straniero 2002).

Since there is no compelling reason to justify the use of a more sophisticated relationship, we have performed a weighted least-squares linear fit of these data, and from a detailed analysis we have found that there is no correlation in this sample between the final masses and metallicity. We have also given some clues on the dependence of the initial-final mass relationship on other parameters, such as rotation and magnetism. In the case of rotation, we have probably found the first evidence that rotation may have in stellar evolution, corroborating that when the progenitor is a fast rotating star, the resulting white dwarf is more

massive, in agreement with the study of Domínguez et al. (1996). Among our sample there are two magnetic white dwarfs with rather different magnetic fields. The masses derived in both cases are also clearly different, being more massive the one with stronger magnetic field. This indicates that the intensity of the magnetic field might be related to the mass of the white dwarf produced. However, given the lack of information on other possible magnetic white dwarfs belonging to this sample, our results are not conclusive enough to assess the impact that magnetic fields may have in the structure of white dwarfs.

In the second part of this work we have tested the initial-final mass relationship by studying its effect on the luminosity function and mass distribution of white dwarfs. For this purpose we have used different stellar evolutionary inputs (stellar tracks and initial-final mass relationships). We have also computed the luminosity function of massive white dwarfs in order to evaluate the impact of the initial-final mass relationship. We have noted some differences between the theoretical luminosity functions, obtaining a clear dependence on the considered initial-final mass relationship, as expected. From a comparison of our results with the observational data from the Palomar Green Survey we have always obtained a reasonable fit when the range of masses was constrained to $M > 0.7\ M_{\odot}$, except when using the initial-final mass relationship of Wood (1992). These calculations were performed assuming a constant star formation rate, but we have also computed the luminosity functions considering an exponentially decreasing star formation rate. We have shown that the production of massive white dwarfs is dependent on the assumed star formation rate, since in the latter case the density of massive white dwarfs drops considerably. Given the presently available observational data, any attempt to discern which initial-final mass relationship better fits the data is not feasible. However, our results favor an initial-final mass relationship that produces more massive white dwarfs than the relation of Wood (1992). This is an important finding, since the initial-final mass relationship of Wood (1992) is the most commonly used relationship for computing the theoretical white dwarf luminosity function.

In the case of the white dwarf mass distribution we have obtained more conclusive results. From a comparison of our results with the observational data available from both the PG survey (Liebert et al. 2005b) and the SDSS (DeGennaro et al. 2008) we have noted that the semi-empirical initial-final mass relationship derived in this work is the one that better fits the central peak of the mass distribution, being in this way very representative of the white dwarf population. On the contrary, the agreement with the observational data is rather poor when the relations of Wood (1992) and Girardi et al. (2002) are considered.

The study carried out in this work evidences the necessity of increasing the number of high quality observations of white dwarfs belonging to stellar clusters, or common proper motion pairs, or to any system that may allow the determination of their total ages and original metallicities with accuracy. On the other hand, this increase in the observational data should be accompanied by refined theoretical studies of the initial-final mass relationship.

ACKNOWLEDGMENTS

We thank the referee, D. Koester for his useful comments and suggestions. We want to thank S. DeGennaro and his collaborators for providing their observational white dwarf mass distribution based on the SDSS data. S.C. acknowledges support from the Spanish Ministerio de Educación y Ciencia (MEC) through a FPU grant. This research was also partially supported by MEC grants AYA05–08013–C03–01 and 02, by the European Union FEDER funds and by the AGAUR.

REFERENCES

Althaus L. G., García-Berro E., Isern J., Córsico A. H., Rohrmann R. D., 2007, A&A, 465, 249A
Aznar Cuadrado R., Jordan S., Napiwotzki R., Schmid H. M., Solanki S. K., Mathys G., 2004, A&A, 423, 1081
Barrado y Navascués D., Stauffer J. R., Bouvier J., Martín E., 2001, ApJ, 555, 546
Bergeron P., Wesemael F., Fontaine G., 1992, ApJ, 387, 288
Catalán S., Isern J., García–Berro E., Ribas I., Allende Prieto C., Bonanos A. Z., 2008, A&A, 477, 213
Claver C. F., Liebert J., Bergeron P., Koester D., 2001, ApJ, 563, 987
Chen L., Hou J. L., Wang J. J., 2003, AJ, 125, 1397
DeGennaro S., von Hippel T., Winget D. E., Kepler S. O., Nitta A., Koester D., Althaus L., 2008, AJ, 135, 1
Díaz-Pinto A., García–Berro E., Hernanz M., Isern J., Mochkovitch R., 1994, A&A, 282, 86
Dobbie P. D., Pinfield D. J., Napiwotzki R., Hambly N. C., Burleigh M. R., Barstow, M. A., Jameson, R. F., Hubeny, I., 2004, MNRAS, 355, L39
Dobbie P. D. et al., 2006, MNRAS, 369, 383
Domínguez I., Straniero O., Tornambé A., Isern I., 1996, ApJ, 472, 783
Domínguez I., Chieffi A., Limongi M., Straniero O., 1999, ApJ, 524, 226
Ferrario L., Wickramasinghe D. T., Liebert J., Williams K. A., 2005, MNRAS, 361, 1131
Fontaine G., Brassard P., Bergeron P., 2001, PASP, 113, 409
García-Berro E., Hernanz M., Mochkovitch R., Isern J., 1988, A&A, 193, 141
García-Berro E., Ritossa C., Iben I., 1997, ApJ, 485, 765
Girardi L., Bertelli G., Bressan A., Chiosi C., Groenewegen M. A. T., Marigo P., Salasnich, B., Weiss, A., 2002, A&A, 391, 195
Hurley J. R., Pols O. R., Tout C. A., 2000, MNRAS, 315, 543
Isern J., García-Berro E., Hernanz M., Mochkovitch R., Torres S., 1998, ApJ, 503, 239
Isern J., Catalán S., García-Berro E., Hernanz M., 2007, in Napiwotzki R. and Burleigh M., eds, ASP Conf. Ser. Vol. 372, 15th European Workshop on White Dwarfs. Astron. Soc. Pac., San Francisco, p. 59
Jeffries G. D., James D. J., Thurston M. R., 1998, MNRAS, 300, 550
Jordan S., Aznar Cuadrado R., Napiwotzki R., Schmid H. M., Solanki S. K. 2007, A&A, 462, 1097

Kalirai J. S., Ventura P., Richer H. B., Fahlman G. G., Durrel P. R., d'Antona F., Marconi G., 2001, AJ, 122, 3239
Kalirai J. S., Richer H. B., Reitzel D., Hansen B. M. S., Rich R. M., Fahlman G. G., Gibson B. K., von Hippel T., 2005, ApJ, 618, 123
Kalirai J. S., Bergeron P., Hansen B. M. S., Kelson D. D., Reitzel D. B., Rich R. M., Richer H. B., 2007, ApJ, 671, 748
Kalirai J. S., Hansen M. S. B., Kelson D. D., Reitzel D. B., Rich R. M., Richer H. B., 2008, ApJ, 676, 594
Kawka A., Vennes S., Wickramasinghe D. T., Schmidt G. D., Koch, R. 2003, in de Martino D., Silvotti R., Solheim J. E., Kalytis R., eds, NATO Science Series II Vol. 105, White Dwarfs. Kluwer Academic Publishers, Dordrecht, p. 109
Kawka A., Vennes S., Schmidt G. D., Wickramasinghe D. T., Koch R. 2007, ApJ, 654, 499
Kepler S. O., Kleinman S. J., Nitta A., et al. 2007, MNRAS, 375, 1315
Kilic M., Stanek K. Z., Pinsonneault M. H., 2007, ApJ, 671, 761
Knox R. A., Hawkins M. R. S., Hambly N. C., 1999, MNRAS, 306, 736
Koester D., Reimers D., 1993, A&A, 275, 479
Koester D., Reimers D., 1996, A&A, 313, 810
Leggett S. K., Ruiz M. T., Bergeron P., 1998, ApJ, 497, 294
Liebert J., Dahn C. C., Monet D. G., 1988, ApJ, 332, 891
Liebert J., Young P. A., Arnett D., Holberg J. B., Williams K. A., 2005a, ApJ, 630, L69
Liebert J., Bergeron P., Holberg J. B., 2005b, ApJS, 156, 47
Marigo P., 2001, A&A, 370, 194
Meynet G., Mermilliod J. C., Maeder A., 1993, A&AS, 98, 477
Moehler S., Koester D., Zoccali M., Ferraro F. R., Heber U., Napiwotzki R., Renzini A., 2004, A&A, 420, 515
Oswalt T., Hintzen P., Luyten W., 1988, ApJS, 66, 391
Oswalt T. D., Smith J. A., Wood M. A., Hintzen P., 1996, Nature, 382, 692
Prada Moroni P. G., Straniero O., 2002, ApJ, 581, 585
Rebolo R., Martin E. L., Magazzu A., 1992, ApJ, 389, 83
Reid I. N., 1996, AJ, 111, 2000
Reimers D., Koester D., 1989, A&A, 218, 118
Reiners A., Schmitt J. H. M. M., 2003, A&A, 412, 813
Richer H. B. et al., 2004, AJ, 127, 2771
Ritossa C., García-Berro E., Iben I., 1996, ApJ, 460, 489
Salaris M., García–Berro E., Hernanz M., Isern J., Saumon D., 2000, ApJ, 544, 1036
Salpeter E. E., 1955, ApJ, 121, 161
Serenelli A. M., Althaus L. G., Rohrmann R. D., Benvenuto O. G., 2002, MNRAS, 337, 1091
Tassoul M., Fontaine G., Winget E. D., 1990, ApJS, 72, 335
Twarog B. A., Ashman K. M., Anthony-Twarog B. J., 1997, AJ, 114, 2556
von Hippel T., 2005, ApJ, 622, 565
Wegner G., 1973, MNRAS, 165, 271
Weidemann V., 1977, A&A, 59, 418
Weidemann V., 2000, A&A, 363, 647
Wickramasinghe D. T., Ferrario L., 2005, MNRAS, 356, 1576
Williams K. A., Bolte M., Koester D., 2004, ApJ, 615, 49
Williams K. A., 2007, in Napiwotzki R. and Burleigh M., eds, ASP Conf. Ser. Vol. 372, 15th European Workshop on White Dwarfs. Astron. Soc. Pac., San Francisco, p. 85
Winget D. E., Hansen, C. J., Liebert J., van Horn H. M., Fontaine G., Nather R. E., Kepler S. O., Lamb D. Q., 1987, ApJ, 315, 77
Wood M. A., 1992, ApJ, 386, 539